International Journal of Modern Physics B
Vol. 28, No. 2 (2014) 1441002 (12 pages)

DOI: 10.1142/S0217979214410021

SYNTHETIC GAUGE FIELDS WITH PHOTONS

M. HAFEZI

Joint Quantum Institute, NIST/University of Maryland, College Park MD, USA
hafezi@umd.edu

Received 31 July 2013
Accepted 5 August 2013
Published 19 November 2013

In this article, we review the recent progress in the implementation of synthetic gauge fields for photons and the investigation of new photonic phenomena, such as nonequilibrium quantum Hall physics. In the first part, we discuss the implementation of magnetic-like Hamiltonians in coupled resonator systems and provide a pedagogical connection between the transfer matrix approach and the couple mode theory to evaluate the system Hamiltonian. In the second part, we discuss the investigation of nonequilibrium fractional quantum Hall physics in photonic systems. In particular, we show that driven strongly interacting photons exhibit interesting many-body behaviors which can be probed using the conventional optical measurement techniques.

Keywords: Topological orders; strongly interacting photons; quantum Hall physics.

PACS number: 03.65.Vf, 42.25.-p, 73.43.Cd

1. Introduction

In his famous 1981 lecture "Simulating physics with computers", Feynman highlighted the impossibility of simulating quantum systems using classical computers. The underlying problem is that the computational power required to describe a quantum system, i.e., the Hilbert space, scales exponentially with the number of its constituents. To overcome this issue, he proposed that a "quantum simulator" is needed that operates according to the laws of quantum mechanics. During the past decade, with the unprecedented degree of control on the light-matter interaction, physicists have been able to implement such ideas in various ultracold gas systems where neutral atoms play the role of the quantum register.[1] Many efforts have been focused on synthesizing magnetic field for neutral atoms to simulate phenomena such as the quantum Hall effects.[2] More recently, photonic systems have been investigated as a new platform to implement such synthetic fields. In particular, there has been an increasing interest in implementing magnetic fields for photons in two dimensions using various techniques: application of strong magnetic field,[3,4] polarization scheme,[5] opto-mechanics,[6] differential optical path,[7–9]

bi-anisotropic metamaterials,[10] harmonic modulation.[11] There has been also recent intriguing progress in side-coupled waveguide systems where the propagation along the waveguide plays the role of time. Examples include: emulation of edge states as localized state at the two ends of a one-dimensional array,[12] topological states in photonic quasi-crystals,[13] strain induced magnetic field[14] and topological Floquet states in helical waveguides.[15] At the same time, there has been efforts to implement synthetic gauge fields in circuit-QED systems.[16,17] In particular, breaking time-reversal symmetry using biased circulators,[18] qubit-assisted tunneling.[19]

In this article, we review the implementation of the synthetic magnetic field in coupled resonator systems. We start by providing a pedagogical connection between the transfer matrix approach and the couple mode theory to evaluate the system Hamiltonian and show that such noninteracting systems can be described by the integer quantum Hall model. Next, we discuss that by adding strong nonlinearity into the system, the system can enter the regime of the fractional quantum Hall physics and its many-body signatures can be probed using the conventional optical measurement techniques.

2. Creating Synthetic Gauge using Coupled Resonators

In this section, we show that the coupled resonators can simulate a magnetic-like Hamiltonian based on differential optical path lengths. In particular, a nonzero magnetic field can be synthesized using an imbalance between the optical paths that connect resonators. In order to show this, we first review the equivalence between the transfer matrix method and the coupled mode theory for two simple systems: a single resonator and a three-resonator system coupled to two probing waveguides. For the three-ring system, we show that the asymmetric coupling of the middle resonator can be described by a nonzero magnetic-phase in the effective Hamiltonian.

We begin by the simplest example: a ring resonator coupled to two waveguides, as shown in Fig. 1(a). In photonics, such system is known as the add/drop filter. We assume that the resonator has a single optical mode. Therefore, using the coupled mode theory (input–output formalism[20]), we can write the dynamics of the field inside the resonator as:

$$\frac{d\mathcal{E}}{dt} = (-\kappa_{\rm in} - 2\kappa_{\rm ex})\mathcal{E} - \sqrt{2\kappa_{\rm ex}}\,\mathcal{E}_{\rm in}e^{-i\omega t}\,, \tag{1}$$

where $\kappa_{\rm ex}$ is the coupling rate between the probing-waveguide and the resonator and $\kappa_{\rm in}$ is the field decay rate to undesired modes. We assumed that a monochromatic field with the amplitude $\mathcal{E}_{\rm in}$ and the detuning ω drives the system, as shown in Fig. 1(a). The output field in the drop port is related to the field inside the resonator by: $\mathcal{E}^{\rm out} = \sqrt{2\kappa_{\rm ex}}\,\mathcal{E}$. Consequently, by solving the dynamics in the Fourier domain, we obtain the transmission in the drop port as:

$$r_{\rm SM} = \frac{\sqrt{2\kappa_{\rm ex}}\,\mathcal{E}}{\mathcal{E}_{\rm in}e^{-i\omega t}} = \frac{2\kappa_{\rm ex}}{i\omega - 2\kappa_{\rm ex} - \kappa_{\rm in}}\,. \tag{2}$$

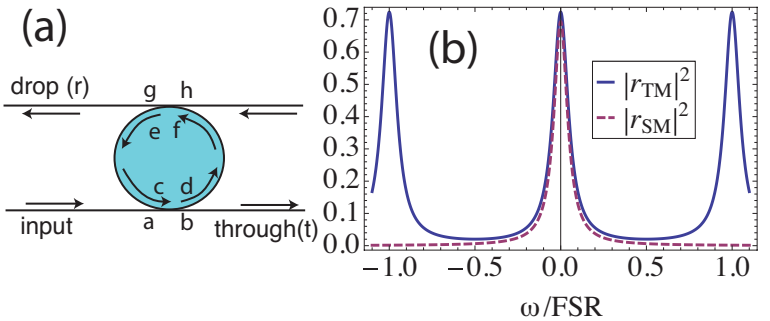

Fig. 1. (a) A resonator connected to two probing waveguides, (b) the transfer matrix formalism and the coupled mode theory yield the same results, for frequencies around the resonance. The parameters are $\epsilon = 0.5$, $\alpha' L = 0.05$.

Now, we evaluate the transmission properties using the transfer matrix formalism. The waveguide-resonator coupling regions can be described as:

$$M_{\text{coupl}} = \frac{1}{t}\begin{pmatrix} -r^2 + t^2 & r \\ -r & 1 \end{pmatrix}, \quad \begin{pmatrix} d \\ c \end{pmatrix} = M_{\text{coupl}} \begin{pmatrix} a \\ b \end{pmatrix}, \quad \begin{pmatrix} g \\ h \end{pmatrix} = M_{\text{coupl}} \begin{pmatrix} f \\ e \end{pmatrix},$$

where t and r are the transmission and reflection coefficients of the coupling regions. Furthermore, we assume that the propagation constant is $\beta = 2\pi n/\lambda$, where n is the index of refraction and λ is the wavelength, and the absorption constant is α'. Therefore, the free propagation inside the resonators is given by:

$$M_{\text{prop}} = \begin{pmatrix} e^{i\beta L/2 - \alpha' L/2} & 0 \\ 0 & e^{-i\beta L/2 + \alpha' L/2} \end{pmatrix}, \quad \begin{pmatrix} f \\ e \end{pmatrix} = M_{\text{prop}} \begin{pmatrix} d \\ c \end{pmatrix}. \tag{3}$$

We are interested in a limit where the coupling loss can be ignored (i.e., $|t|^2 + |r|^2 = 1$) and the junctions are highly reflective. In other words: $r \to \sqrt{1-\epsilon^2}$, $t \to i\epsilon$, where $\epsilon \ll 1$. The regime of interest is near the resonant frequency of the resonator, and is much smaller than the free spectral range (FSR), so we consider $\beta L \ll 1$. Since the propagation loss over a typical distance in these systems is not large, we take $\alpha' L \ll 1$. The input field is only present at one port, as shown in Fig. 1(a), so we can replace: $a = 1$, $h = 0$. Keeping terms to the total 2nd order in ϵ^2, βL, $\alpha' L$, both in the numerator and the denominator, we find that the field in the drop channel can be simplified as:

$$r_{\text{SM}} = \frac{\epsilon^2}{i\beta L - \alpha' L - \epsilon^2}. \tag{4}$$

Now, if we use the following substitutions:

$$\epsilon^2 \to \frac{4\pi\kappa_{\text{ex}}}{\text{FSR}}, \quad \alpha' L \to \frac{2\pi\kappa_{\text{in}}}{\text{FSR}}, \quad \beta L \to 2\pi\frac{\omega}{\text{FSR}}, \tag{5}$$

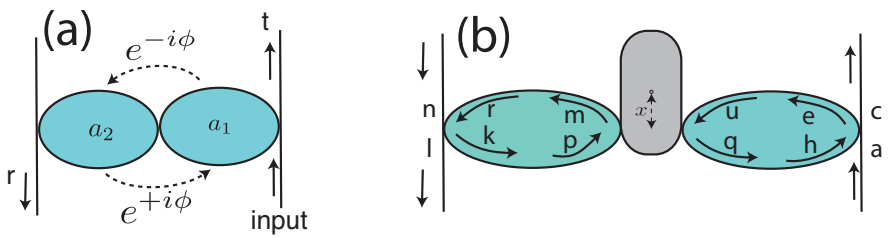

Fig. 2. (a) Two ring resonator coupled with a hopping phase (ϕ). (b) Two ring resonators coupled through an off-resonant middle ring. These two systems are equivalent around the resonant frequency of side resonators.

we see that Eqs. (4) and (2) are equivalent. One can also compare these two approaches, using the exact expressions, as shown in Fig. 1(b). Both formalism agree with each other around the resonant frequency.

In the following, we show that the dynamics of two ring resonators that are coupled through a middle off-resonant ring can be effectively written as two resonators coupled with a "hopping phase". We evaluate transport properties in both cases and show that they are identical, around the resonant frequency of the side resonators.

First, we derive the transmission and reflection coefficients of two rings coupled with a hopping phase. The Hamiltonian describing such system can be written as:

$$H = -J\hat{a}_2^\dagger \hat{a}_1 e^{-i\phi} - J\hat{a}_1^\dagger \hat{a}_2 e^{+i\phi}\,, \tag{6}$$

where J is the tunneling rate and ϕ is the hopping phase, as depicted in Fig. 2(a). Note that by hopping phase we mean a Hamiltonian of the kind written in Eq. (6). This should not be confused with optical nonreciprocity which requires an external field, cf. Refs. 6 and 11. Similar to the single resonator case, using coupled mode theory, we can write the dynamics of the field inside the resonators as:

$$\frac{d}{dt}\begin{pmatrix} a_1 \\ a_2 \end{pmatrix} = \begin{pmatrix} -\kappa_{\rm in}-\kappa_{\rm ex} & iJe^{+I\phi} \\ iJe^{-I\phi} & -\kappa_{\rm in}-\kappa_{\rm ex} \end{pmatrix}\begin{pmatrix} a_1 \\ a_2 \end{pmatrix} - \sqrt{2\kappa_{\rm ex}}\begin{pmatrix} \mathcal{E}_{\rm in} \\ 0 \end{pmatrix}. \tag{7}$$

The output field of the resonators is given by: $a_2^{\rm out} = \sqrt{2\kappa_{\rm ex}}\,a_2$, $a_1^{\rm out} = 1+\sqrt{2\kappa_{\rm ex}}\,a_1$. Consequently, the transmission and reflection coefficients, as defined in Fig. 2, are given by:

$$\begin{aligned} r_{\rm SM} &= \frac{\sqrt{2\kappa_{\rm ex}}\,a_2}{\mathcal{E}_{\rm in}} = -\frac{2ie^{-i\phi}J\kappa_{\rm ex}}{J^2+(i\omega-\kappa_{\rm ex}-\kappa_{\rm in})^2}\,, \\ t_{\rm SM} &= \frac{\sqrt{2\kappa_{\rm ex}}\,a_1+1}{\mathcal{E}_{\rm in}} = 1+\frac{2\kappa_{\rm ex}(+i\omega-\kappa_{\rm ex}-\kappa_{\rm in})}{J^2+(+i\omega-\kappa_{\rm ex}-\kappa_{\rm in})^2}\,. \end{aligned} \tag{8}$$

Now, we consider two ring resonators that are coupled through a middle off-resonant ring, as shown in Fig. 1(b). We use the transfer matrix formalism to derive the transmission of the system. The transfer matrix for the waveguide-resonator and

resonator–resonator coupling regions, respectively, are given by:

$$M_1 = \frac{1}{t_1}\begin{pmatrix} -r_1^2 + t_1^2 & r_1 \\ -r_1 & 1 \end{pmatrix},$$

$$M_2 = \frac{1}{t_2}\begin{pmatrix} -r_2^2 + t_2^2 & r_2 \\ -r_2 & 1 \end{pmatrix},$$

where t_i and r_i are the transmission and reflection coefficients of the coupling regions. Therefore, the waveguide-resonator couplings can be written as:

$$\begin{pmatrix} e \\ h \end{pmatrix} = M_1 \begin{pmatrix} a \\ c \end{pmatrix}, \quad \begin{pmatrix} l \\ s \end{pmatrix} = M_1 \begin{pmatrix} r \\ k \end{pmatrix}. \tag{9}$$

We assume that the length of the side resonators (the middle resonator) is L ($L+\eta$), so that the middle resonator remains off-resonant with the other two. Furthermore, the middle resonator is shifted vertically by x to induce the hopping phase, as we show. Therefore, the free propagation inside the side resonators is described by Eq. (3). The propagation inside the middle rings is given by:

$$\begin{pmatrix} m \\ p \end{pmatrix} = M_2 \begin{pmatrix} e^{i\beta L/2 + i\beta\eta - i2\beta x - \alpha' L/2} & 0 \\ 0 & e^{-i\beta L/2 - i\beta\eta - i2\beta x + \alpha' L/2} \end{pmatrix} M_2 \begin{pmatrix} u \\ q \end{pmatrix}. \tag{10}$$

Again, keeping terms to the total 2nd order in ϵ_i^2, βL, $\alpha' L$, we find that the field in the drop channel can be simplified as:

$$r_{\mathrm{TM}} = \frac{2e^{-i\beta x}\epsilon_1^2\epsilon_2^2}{2(2\alpha' L - 2i\beta L + \epsilon_1^2)\epsilon_2^2\cos(\beta\eta) - i((2\alpha' L - 2i\beta L + \epsilon_1^2)^2 + \epsilon_2^4)\sin(\beta\eta)}. \tag{11}$$

To compare this expression with the one obtained from the single-mode approximation [Eq. (8)], we use the following substitutions:

$$\epsilon_1^2 \to \frac{4\pi\kappa_{\mathrm{ex}}}{\mathrm{FSR}}, \quad \epsilon_2^2 \to \frac{4\pi J}{\mathrm{FSR}}, \quad \alpha' L \to \frac{2\pi\kappa_{\mathrm{in}}}{\mathrm{FSR}}, \quad \beta L \to 2\pi\frac{\omega}{\mathrm{FSR}}, \quad \beta x \to \phi \tag{12}$$

and we have

$$r_{\mathrm{TM}} = \frac{2e^{-i\phi}J\kappa_{\mathrm{ex}}}{2J(\kappa_{\mathrm{ex}} + \kappa_{\mathrm{in}} - i\omega)\cos(\beta\eta) - i(J^2 + (\kappa_{\mathrm{ex}} + \kappa_{\mathrm{in}} - i\omega)^2)\sin(\beta\eta)}. \tag{13}$$

In the special case where $\beta\eta = 3\pi/2$, this expression reduces to Eq. (8). This means that if the middle ring is precisely anti-resonant with the side rings, the three rings can be effectively described by two resonators coupled with a hopping phase. If we have $\beta\eta = \pi/2$, the two models are again the same, only the sign of the tunneling is reversed ($J \to -J$). When the middle resonator deviates from the anti-resonant condition ($\beta\eta = \pi/2, 3\pi/2, \ldots$), the system can still be effectively described by two resonators with a hopping phase, however, the effective tunneling is $J_{\mathrm{eff}} \to J/\sin(\beta\eta)$ and system is shifted in frequency by $\omega \to \omega - J\cot(\beta\eta)$.

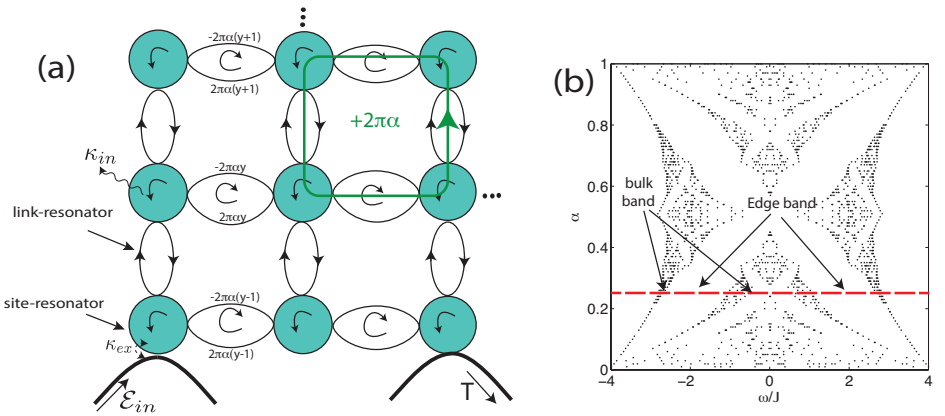

Fig. 3. (Color online) (a) A 2D lattice of coupled resonators which is described by a magnetic tight-binding model [Eq. (14)], (b) Hofstadter butterfly spectrum. Each point represents a transmission greater than 0.005, for a 10×10 lattice with torus boundary condition and coupling $\kappa_{\rm ex}/J = 0.02$. The red line is a guide for the eye to show the spectrum at the specific magnetic field ($\alpha = 0.25$). The bulk and edge band are highlighted.

Now, we consider a two-dimensional system of coupled resonators, where two sets of resonators play the role of sites and links of a lattice, as shown in Fig. 3. We arrange the system so that the phase imbalance is only present in the row link-resonator and increases by the row number. The dynamics of the system near the resonance of the site resonators is described by the following Hamiltonian

$$H_{\rm mag} = -J \sum_{x,y} \hat{a}^\dagger_{x+1,y} \hat{a}_{x,y} e^{i2\pi\alpha y} + \hat{a}^\dagger_{x,y} \hat{a}_{x+1,y} e^{-i2\pi\alpha y} + \hat{a}^\dagger_{x,y+1} \hat{a}_{x,y} + \hat{a}^\dagger_{x,y} \hat{a}_{x,y+1} \,, \tag{14}$$

where $a^\dagger_{x,y}$ is the creation operator at site (x, y), J is the effective tunneling rate between resonators and α characterizes the phase imbalance. In particular, a photon hopping around a plaquette, in the counter-clockwise direction, acquires the phase $2\pi\alpha$, in direct analogy to Aharanov–Bohm phase. Therefore, α is the effective magnetic flux per plaquette and the total magnetic flux is $N_\phi = \alpha N_x N_y$.

In this discussion, we assumed only counter-clockwise photons in the site- (link-) resonators. The opposite circulating photon experience the opposite magnetic field. Therefore, the system is equivalent to two copies of integer quantum Hall systems with opposite magnetic fields, in direct analogy to a special case of the quantum spin Hall physics in electronic systems.[21]

The Hamiltonian in Eq. (14) is identical to that of an electron on a lattice with a uniform magnetic field and the spectrum of the system is known as the Hofstadter butterfly, when $N_x, N_y \to \infty$. The spectrum of such photonic system can be probed using transmission spectroscopy. By applying the input–output formalism, we can evaluate different transport coefficients. In this section, the dynamics is linear, therefore, the "quantum" input–output formalism reduces to the "classical"

coupled mode theory, by replacing the field operator with the corresponding expectation value, i.e., $\langle \hat{a}_{x,y} \rangle = a_{x,y}$. The field dynamics of the resonators is given by:

$$\frac{d\hat{a}_{x,y}}{dt} = i[H, \hat{a}_{x,y}] + [-\kappa_{\text{in}} - \kappa_{\text{ex}}(\delta_{x,x_{\text{in}}}\delta_{y,y_{\text{in}}} + \delta_{x,x_{out}}\delta_{y,y_{out}})]\hat{a}_{x,y} - \sqrt{2\kappa_{\text{ex}}}\,(\delta_{x,x_{\text{in}}}\delta_{y,y_{\text{in}}})\mathcal{E}_{\text{in}}e^{-i\omega t}\,, \tag{15}$$

where κ_{ex} is the coupling rate between the probing-waveguide and the site resonators and κ_{in} is the field decay rate to undesired modes. "In" ("out") represents the resonators to which the input (output) probing waveguides are connected. We assume a monochromatic input field at the left-bottom corner resonator, with amplitude $\mathcal{E}_{\text{in}}$ and detuned by ω from the resonance, as shown in Fig. 3(a). Going to the Fourier domain and evaluating the steady-state solution, we can obtain the transmission in the output channel as $T = |a_{x_{\text{out}},y_{\text{out}}}/\mathcal{E}_{\text{in}}|^2$.

Since an infinite system can be simulated by a finite system with periodic boundary condition, we study a 10×10 lattice with torus boundary condition. Figure 3(b), shows the transmission profile when the magnetic flux varies from 0 to 2π. We observe that a finite version of the Hofstadter's fractal appears.

In a finite lattice, there exist states between magnetic bulk bands which are known as "edge states". In direct analogy to quantum Hall physics, such quasi one-dimensional states localized at the perimeter of the system which carry current. In particular, for certain frequency bands, the field in resonators located in the bulk (away from the edges) undergoes destructive interference and, therefore, the light intensity is nonzero only at the edges. This is illustrated in Fig. 4(a). For each edge state, there is a corresponding edge state with an opposite chirality. More specifically, the forward- and backward-propagating edge states take different paths, and consequently, they have different resonances at detunings, equal in magnitude and opposite in sign.

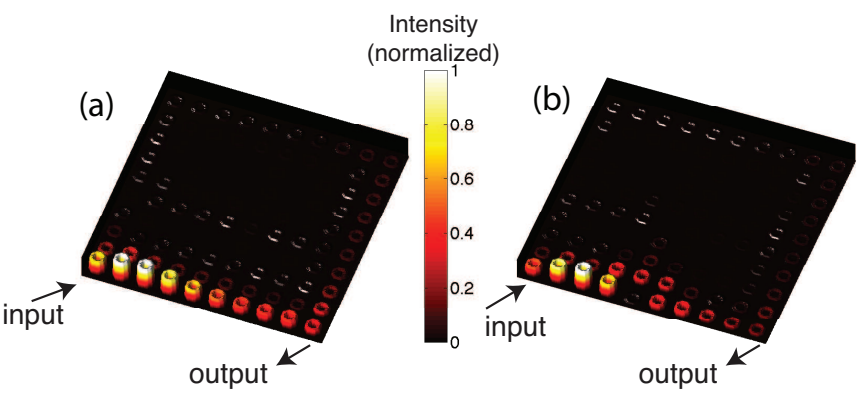

Fig. 4. Light intensity for a 10×10 lattice (a) in the absence and (b) in the presence of disorder. For (b) the resonator $(x, y) = (5, 1)$ is detuned by $U = 20\ J$. For both figures, the parameters are: $(\kappa_{\text{ex}}, \kappa_{\text{in}})/J = 0.2, 0.1, \alpha = 0.25$ and the system is excited at $\omega = 2\ J$.

Again in direct analogy to integer quantum Hall edge state, such edge states are immune to disorders in the form of random potential. In particular, when an impurity is located on the edge — the resonator is detuned ($U\hat{a}^{\dagger}_{x,y}\hat{a}_{x,y}$) — the edge state routes around it, as shown in Fig. 4(b) for the test case of a single disordered site. More precisely, scattering which would reverse the current is prevented because the backward going edge state has a different energy, as discussed above, preventing elastic scattering.

Transport through edge states requires the photon to traverse the perimeter of the system, leading to a time delay proportional to the transverse resonators. Since such transport is robust against frequency mismatch of among resonators, such two-dimensional systems provide a robust alternative to conventional CROW in photonic delay lines.[7]

3. Nonequilibrium Fractional Quantum Hall Physics

In this section, we show that the above system can be extended to investigate strongly interacting photonic states. In particular, by inducing strong photon–photon interaction, we show that certain fractional quantum Hall states can be generated, and their signature can be probed using the correlation function measurement.

Photon–photon interaction can be mediated by coupling emitters (e.g., atoms) to each resonator, as shown in Fig. 5. In the strong coupling regime, where the photon blockade is observed,[22–24] this interaction can be represented as an on-site interaction in a Bose–Hubbard model for a coupled array of resonators.[25–27] As

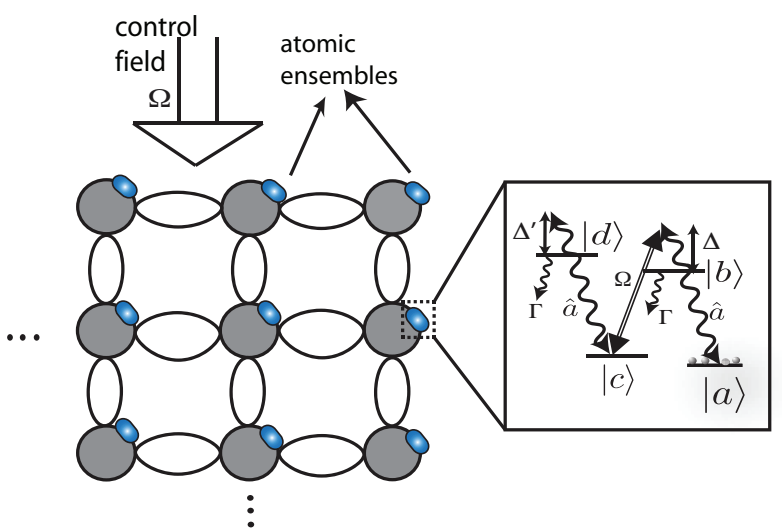

Fig. 5. Atomic ensembles are coupled to resonators to mediate interaction. Inset: Mediating interaction using N-level atomic ensemble. A control field couples the internal levels, and provides on-site interaction for photons.

shown in Refs. 28–31, in the presence of a synthetic magnetic field, such interacting system of photons can be described by a Hamiltonian which is identical to the fractional quantum Hall Hamiltonian on a lattice:

$$H_{\rm mag} = -J\sum_{x,y} \hat{a}^{\dagger}_{x+1,y}\hat{a}_{x,y}e^{i2\pi\alpha y} + \hat{a}^{\dagger}_{x,y}\hat{a}_{x+1,y}e^{-i2\pi\alpha y} + \hat{a}^{\dagger}_{x,y+1}\hat{a}_{x,y} + \hat{a}^{\dagger}_{x,y}\hat{a}_{x,y+1} + U\hat{a}^{\dagger}_{x,y}\hat{a}_{x,y}(\hat{a}^{\dagger}_{x,y}\hat{a}_{x,y} - 1)\,. \quad (16)$$

Such Hamiltonian can be implemented by adding strong optical nonlinearity in the scheme presented in the previous section. As an example case, one can use an ensemble of N-level atoms to mediate onsite two-body interaction of the Kerr-type (Fig. 5),[26] which still preserves the propagation direction (clockwise or counterclockwise) used in Ref. 7. In this approach, the optical cavity and ensemble enter into a slow-light regime, where the excitations are dark state polaritons[32] $\hat{\Psi}_{x,y} \propto \Omega\hat{a}_{x,y} - g\sqrt{N}\hat{S}_{x,y}$, where Ω is the pump field, g is the vacuum Rabi coupling, N is the number of ensemble atoms and $\hat{S}_{x,y}$ is the spin-wave operator describing coherence between two atomic states $|a\rangle$ and $|c\rangle$ (from Fig. 5 inset). These bosonic excitations lead to an overall increase of dynamical timescales by $\eta = c/v_g \gg 1$, the ratio between the speed of light and group velocity for the dark state polariton, but they can also interact via a self-Kerr interaction with state $|d\rangle$.[33] Coupling atoms to the photonic system introduces loss which can be reduced by detuning the cavity resonance from the emitter transitions ($\Delta, \Delta' \gg \Gamma$). As discussed in Ref. 34, to observe any many-body effect and to have a finite gap, the effective interaction between photons ($U \simeq g^2/\Delta'$) should be at least comparable to the tunneling rate J. These conditions can be satisfied for systems with a large Purcell factor ($g^2/\kappa\Gamma \gg 1$). The same criterion applies to implementation of such scheme in the microwave domain.

Following Refs. 34 and 35, the ground state of Eq. (16) are the fractional quantum Hall states when the magnetic field is dilute ($\alpha < 0.4$). In particular, when the filling factor ($\nu = N_{\rm ph}/N_{\phi}$), which is the ratio between the number of photons ($N_{\rm ph}$) and the total magnetic field $N_{\phi} = \alpha N_x N_y$, is one half, the ground state of the system can be faithfully described by Laughlin wavefunction ($\alpha < 0.25$). For numerical simulation, one has to consider a torus boundary condition to mimic the effect of an infinite system. One a torus, the Laughlin wavefunction is written using the Jacobi theta function. The detailed discussion of the overlap calculation can be found in Ref. 34. The remarkable overlap with the Laughlin state in the photonic case is discussed in Refs. 28–31.

One can prepare a Laughlin state by adiabatically melting a Mott-insulator of photons, similar to the atomic method discussed in Ref. 35. However, this requires both preparation of $N_{\rm ph}$ Fock states and photon lifetimes long enough to allow for the melting to be adiabatic. Moreover, the direct experimental verification of the Laughlin overlap is a difficult task which requires number post-selection ($N_{\rm ph}$) and state tomography in a Hilbert space with dimension $\binom{N_x N_y}{N_{\rm ph}}$. Therefore, it is

important to find an implementation and a detection scheme that is more relevant for photonic system.

More generally most of the studies in many-body photonic system is inspired by analogies to electronic systems which are mainly focused on ground state properties. However, a photonic system is naturally an open driven system. Therefore, the most relevant approach to understand and manipulate many-photon states involves understanding the nonequilibrium dynamics in such systems.[36–41] For example, in a one-dimensional system strong interaction between photons leads to their fermionization, which can be probed in the output correlation functions of an externally driven system, both in a discrete array[36] and in the continuum limit.[38]

For the fractional quantum Hall system, Ref. 31 demonstrates that by weakly driving the system, a few photon Laughlin state can be prepared and experimentally-relevant observables such as the correlation function of the zero-mode can show certain signatures of the Laughlin state. Since the system is driven and lossy, it may seem that the master equation formalism is required to fully described the system. However, as shown in Ref. 31, when the system is weakly driven, one can resort to the stochastic wavefunction approach. More precisely, if we are interested in evaluating the correlation function of any order, finding the steady-state of the effective Hamiltonian is sufficient and the effect of the "quantum jumps" can be ignored. Such simplification allows one to explore larger systems, compared to the master equation approach, and to avoid finite size effects, which usually undermines the numerical results.

When all the resonators are driven with a laser field, the input field consists of a Poisson distribution of photons. When photons are injected at the frequency corresponding to the Laughlin state at the $N_{\rm ph}$-photon manifold, photons reconfigure

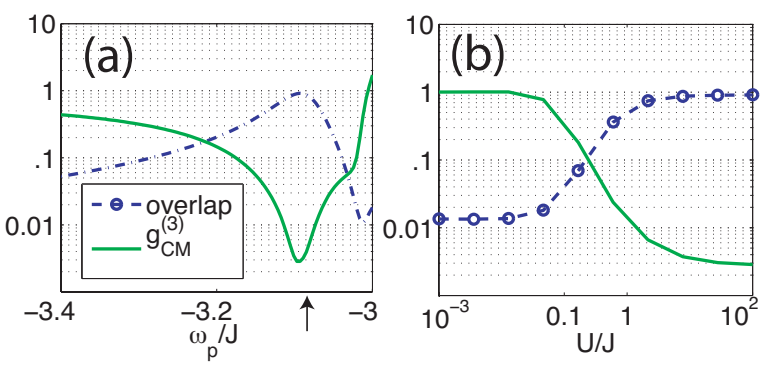

Fig. 6. Overlap with the Laughlin wavefunction ($\nu = 1/2$), and the correlation function of the zero mode ($g^{(3)}_{CM}$) are shown as a function of: (a) the pump frequency for hard-core bosons (b) the interaction strength for $\Delta = -3.095\ J$, as shown by an arrow on (a). The overlap with the Laughlin function is evaluated for $N_{\rm ph} = 3$ manifold. The total magnetic flux is $N_\phi = 6$. The simulations are performed for a 6×6 lattice, torus boundary condition and the maximum number of photon is 3. $\kappa = 0.01\ J$, $\beta = 0.01$. All calculated quantities are dimensionless. Figures are reproduced from Ref. 13.

themselves and form a wavefunction which corresponds to the Laughlin state. The remarkable overlap of this photonic state with the Laughlin wavefunction in the $N_{\rm ph}$-photon manifold is shown in Fig. 6(a). Note the frequency required to be resonant with the Laughlin state is at the vicinity of the free photon state (Hofstadter's spectrum). We can relax the hard-core constraint and investigate the same observables. In the weak interaction limit, the system approaches the classical response, as shown in Fig. 6(b). In the absence of interaction, using transport measurements — varying the pump frequency and measuring reflection/transmission — one recovers the Hofstadter's butterfly spectrum as in Fig. 3(b), but regardless of the pump frequency, the correlation function remains equal to one.

To summarize, the driven strongly interacting photons exhibits interesting many-body behaviors and the emergence of FQH states of photons can be probed by using the conventional optical measurement techniques. One of the remaining question is to investigate other many-body signatures of these states such as their topological properties and fractional statistics.

4. Outlook

As we briefly discussed in this review, there are promising platforms to investigate synthetic gauge fields in the optical domain. The advantage in the optical domain is the relative ease of implementing the synthetic gauge fields and the possibility of performing the experiments on the noninteracting models at room temperature. However, the challenge in the optical domain remains to be the weakness of nonlinearity and the difficulties in reaching photon-blockade on each resonators without inducing any inhomogeneity.

On the other hand, there has been recent investigation in the microwave domain to implement synthetic gauge field[18,19] and explore many-body effects.[42] The advantage in the microwave domain is the presence of strong nonlinearity provided by the Josephson junctions. However, the challenges are the operation at very low temperature which requires dilution fridges and the presence of inhomogeneity in fabricated arrays of qubits.

In both cases, due to the open nature of photonic systems, preparation and detection should be performed in a driven regime. This arises many interesting theoretical questions to investigate many-body features such as incompressibility, fractional statistics in nonequilibrium systems. For example, new effective field theories should be developed to treat excitations in such bosonic systems. An intriguing bright future awaits for theoretical and experimental investigation of many-body physics, both in the optical and the microwave domains.

References

1. I. Bloch, J. Dalibard and W. Zwerger, *Rev. Mod. Phys.* **80**, 885 (2008).
2. J. Dalibard, F. Gerbier, G. Juzeliūnas and P. Öhberg, *Rev. Mod. Phys.* **83**, 1523 (2011).

3. F. Haldane and S. Raghu, *Phys. Rev. Lett.* **100**, 13904 (2008).
4. Z. Wang, Y. Chong, J. D. Joannopoulos and M. Solja Ccaron I Cacute, *Nature* **461**, 772 (2009).
5. R. O. Umucalilar and I. Carusotto, *Phys. Rev. A* **84**, 043804 (2011).
6. M. Hafezi and P. Rabl, *Opt. Expr.* **20**, 7672 (2012).
7. M. Hafezi, E. A. Demler, M. D. Lukin and J. M. Taylor, *Nat. Phys.* **7**, 907 (2011).
8. M. Hafezi, J. Fan, A. Migdall and J. Taylor, to appear in *Nat. Photon.*
9. G. Q. Liang and Y. D. Chong, *Phys. Rev. Lett.* **110**, 203904 (2013).
10. A. B. Khanikaev *et al.*, *Nat. Mater.* **12**, 233 (2013).
11. K. Fang, Z. Yu and S. Fan, *Nat. Photon.* **6**, 782 (2012).
12. Y. Kraus *et al.*, *Phys. Rev Lett.* **109**, 106402 (2012).
13. M. Verbin *et al.*, *Phys. Rev. Lett.* **110**, 076403 (2013).
14. M. C. Rechtsman *et al.*, *Nat. Photon.* **7**, 153 (2013).
15. M. C. Rechtsman *et al.*, *Nature* **496**, 196 (2013).
16. R. J. Schoelkopf and S. M. Girvin, *Nature* **451**, 664 (2008).
17. M. H. Devoret and R. J. Schoelkopf, *Science* **339**, 1169 (2013).
18. J. Koch *et al.*, *Phys. Rev. A* **82**, 043811 (2010).
19. E. Kapit, arXiv:1302.6596v1.
20. C. W. Gardiner and M. J. Collett, *Phys. Rev. A* **31**, 3761 (1985).
21. B. Bernevig and S.-C. Zhang, *Phys. Rev. Lett.* **96**, 106802 (2006).
22. K. M. Birnbaum *et al.*, *Nature* **436**, 87 (2005).
23. D. Englund *et al.*, *Nature* **450**, 857 (2007).
24. K. Srinivasan and O. Painter, *Nature* **450**, 862 (2007).
25. A. D. Greentree *et al.*, *Nat. Phys.* **2**, 856 (2006).
26. M. J. Hartmann, F. G. S. L. Brandao and M. B. Plenio, *Nat. Phys.* **2**, 849 (2006).
27. D. Angelakis, M. Santos and S. Bose, *Phys. Rev. A* **76**, 31805 (2007).
28. J. Cho, D. Angelakis, and S. Bose, *Phys. Rev. Lett.* **101**, 246809 (2008).
29. R. O. Umucalilar and I. Carusotto, *Phys. Rev. Lett.* **108**, 206809 (2012).
30. A. L. C. Hayward, A. M. Martin and A. D. Greentree, *Phys. Rev. Lett.* **108**, 223602 (2012).
31. M. Hafezi, M. D. Lukin and J. M. Taylor, *New J. Phys.* **15**, 063001 (2013).
32. M. Fleischhauer and M. D. Lukin, *Phys. Rev. Lett.* **84**, 5094 (2000).
33. A. Andre *et al.*, *Phys. Rev. Lett.* **94**, 063902 (2005).
34. M. Hafezi *et al.*, *Phys. Rev. A* **76**, 023613 (2007).
35. A. S. Sorensen, E. Demler and M. D. Lukin, *Phys. Rev. Lett.* **94**, 086803 (2005).
36. I. Carusotto *et al.*, *Phys. Rev. Lett.* **103**, 033601 (2009).
37. A. Tomadin *et al.*, *Phys. Rev. A* **81**, 061801 (2010).
38. M. Hafezi *et al.*, *Europhys. Lett.* **94**, 54006 (2011).
39. A. Nunnenkamp, J. Koch and S. M. Girvin, *New J. Phys.* **13**, 095008 (2011).
40. F. Nissen *et al.*, *Phys. Rev. Lett.* **108**, 233603 (2012).
41. M. Schiró *et al.*, *Phys. Rev. Lett.* **109**, 053601 (2012).
42. A. A. Houck, H. Tureci and J. Koch, *Nat. Phys.* **8**, 292 (2012).